Surface Properties of the Ethanol/Water Mixture: Thickness and Composition

Anita E. Hyde[1], Maho Ohshio[2], Cuong V. Nguyen[1], Shin-ichi Yusa[2], Norifumi L. Yamada[3] and Chi M. Phan[1]

[1]Department of Chemical Engineering and Curtin Institute of Functional Molecules and Interfaces, Curtin University, GPO Box U1987, Perth, WA 6845, Australia

[2]Graduate School of Engineering, University of Hyogo, 2167, Shosha, Himeji 671-2280, Japan

[3]Institute of Material Structure Science, High Energy Accelerator Research Organization (KEK), Tokai, Naka, Ibaraki 319-1106, Japan

Keywords: Ethanol/water mixture; Surface adsorption; Neutron reflectivity

ABSTRACT

Ethanol is a common amphiphilic solvent, often used in conjunction with water. However, despite its widespread use, key questions regarding the thickness and composition of molecules at the ethanol/water/air surface remain unclear. Recent thermodynamic analyses, Bagheri and co-authors (2016) and Santos and Reis (2018), indicated that the interfacial thickness is not constant. However, the interfacial thickness from these two analyses follows opposite trends. This study aims to provide a detailed description of the thickness and composition of the interfacial layer by combining neutron reflectivity (NR) experiments with rigorous molecular simulation. The

interfacial composition was determined from molecular simulations and, in conjunction with the Gibb's excess concentration, used to calculate the interfacial thickness. It was found that the thickness decreased exponentially and reached a plateau of ~ 8.2 Å. The results confirm the trends obtained thermodynamically from surface tension. The study also provides a new theoretical framework to describe the interfacial layer of water/alcohol mixtures.

INTRODUCTION

As with all alcohols, ethanol combines a hydrophilic head with a non-polar tail, leading to a weakly amphiphilic molecule [1,2]. As such, ethanol tends to enrich at the water/air interface and its concentration in the surface layer can be significantly higher than found in the bulk [3]. Due to its properties in the bulk and at the surface, ethanol can be classified as either solvent or co-surfactant [4]. While this fact has well-accepted since the early 20th century, the actual surface concentration is difficult to quantify, for two key reasons:

(1) The surface concentration cannot be directly measured, and

(2) The interfacial layer itself is poorly defined and cannot be physically measured.

Many models attempting to describe the phenomena of ethanol adsorption have been proposed in the literature [5–7] . Most of these models were developed to explain the behaviour of the mixture's surface tension. One such model, the Gibbs adsorption equation, is the common means to calculate the relative absorption of a species at the interface [5,6]. A surfactant solution is often characterised by the Gibbs surface excess concentration, $\Gamma_e^{(w)}$ [7,8]. Rather than being an exact concentration, the Gibbs excess is a relative value that describes the difference between the concentrations in the interfacial and bulk regions. However, $\Gamma_e^{(w)}$ is defined with reference to an

arbitrary surface, the Gibbs dividing plane. Consequently, the Gibbs excess concentration can offer little insight into the physical properties of the interfacial layer. Calculation of a molar surface concentration (from the Gibbs excess) is possible only through the use of an additional physical constraint, [9] such as the thickness of the interface. While this method is often used as an estimate, the approach suffers a considerable setback. Namely, that there is currently no way to physically measure the interfacial thickness. Various models have been developed from molar-[10] and volume-[11] weighted averages, statistical mechanics[12] and density functional theory [13] to describe the surface layer of ethanol/water mixture based on the Gibbs excess.

Conventionally, it was assumed that alcohols formed a monolayer at the water/air interface [5]. Consequently, the interfacial thickness was expected to reach a constant value roughly in line with the length of the alcohol. By modelling the molecule as a cylinder with its vertical axis lying perpendicular to the interface, it was estimated that the minimum area that could be allocated to each molecule (i.e. the surface area per molecule) was on the order of 20 $Å^2$ [5]. Furthermore, as it was the charged heads that were thought to be the limiting factor in such an arrangement, all straight-chain alcohols were predicted to have roughly the same maximum surface coverage, corresponding to a Gibbs surface excess concentration of 0.8×10^{-6} mol/m^2.[5]

Recent thermodynamic analyses [1,2] have advanced the description of the ethanol/water interfacial layer. Most importantly, these analyses show that the interfacial thickness is not constant. For the ethanol/water mixture, Bagheri and co-authors [1] have demonstrated that the interfacial thickness decreases with increasing ethanol concentration. This is contrasting to the analysis of Santos and Reis [2], which showed an increasing thickness over the same concentration range. Furthermore, these studies showed that the Gibbs excess concentration is not limited to 0.8×10^{-6} mol/m^2, and thus that the enrichment of alcohol at the water/air interface is not limited to a

monolayer. These conflicting results demand further investigation independent of surface tension data.

This study investigates the ethanol/water interfacial layer by neutron reflectivity (NR) to directly measure the change in neutron scattering across the interfacial layer, and molecular simulations. To the best of the authors' knowledge, the only research claiming to have measured the interfacial adsorption of ethanol in water by NR was published by Li et al [14] in 1993. With the significant advances in measuring and modelling capabilities, NR has the potential to offer new insights into the molecular arrangements at the ethanol/water/air interface. Specifically, this study aims to quantify the variation in interfacial thickness and composition. As the interfacial thickness cannot be measured experimentally, its length being on the same scale as the measured roughness of the pure water/air surface [15], it is a property that can only be inferred from other measurements. Furthermore, it is strongly dependent on the definition of the boundaries of the interfacial region. The combination of NR analysis and molecular simulations provides a more objective view of the interfacial region. The results, in combination with molecular simulations, clarify contradicting hypotheses in the literature. This new knowledge allows better prediction of the interfacial properties for application to alcohol/water mixtures.

THEORY

In this section, we provide a methodology to calculate the interfacial composition from the Gibbs excess concentration, $\Gamma_e^{(w)}$, for a known bulk concentration, x_e^b, and a given interfacial thickness, δ. In the following analysis, subscripts ‘e’ and ‘w’ represent ethanol and water, and the superscripts ‘b’ and ‘s’ represent the bulk and surface layers, respectively.

Consider an interface of thickness δ and unitary area, A (1 cm^2), with the corresponding interfacial volume, $V = \delta A$. The volume of the interfacial layer can be described as a function of the partial molar volumes, v_w and v_e, of the liquid components, and their respective number of mole (n) inside the interfacial zone:

$$n_w^s v_w + n_e^s v_e = V \quad n_w^s v_w + n_e^s v_e = V \tag{1}$$

Or

$$N_w^s v_w + N_e^s v_e = 1 \tag{2}$$

Where the molar concentrations, N_i, represent the concentration of each species (i) in the interfacial volume:

$$N_i^s = \frac{n_i^s}{V} \tag{3}$$

The partial molar volumes were calculated as described by [16] from published data [17]. The molar fractions of ethanol in the bulk and interfacial zones can be defined as follows:

$$x_e^s = \frac{N_e^s}{N_e^s + N_w^s} \tag{4}$$

$$x_e^b = \frac{N_e^b}{N_e^b + N_w^b} \tag{5}$$

We define N_e^{BE} ("bulk equivalent") as the concentration of solute that would be expected if the molar fractions in the bulk and interfacial layers were equivalent. Consequently:

$$N_e^{BE} = \frac{x_e^b}{1 - x_e^b} N_w^s \tag{6}$$

The Gibbs relative surface excess is the two-dimensional concentration *in excess* of this "equivalent" bulk concentration. Hence:

$$\Gamma_e^{(w)} = N_e^s \delta - N_e^{BE} \delta \tag{7}$$

The total ethanol concentration in the interfacial layer is then expressed as:

$$N_e^s = \frac{\Gamma_e^{(w)}}{\delta} + \frac{x_e^b}{1 - x_e^b} N_w^s \tag{8}$$

The concentration of water in the interfacial layer can be determined by combining eqs. (2) and (8) as follows:

$$N_w^s v_w + \left(\frac{\Gamma_e^{(w)}}{\delta} + \frac{x_e^b}{1 - x_e^b} N_w^s \right) v_e = 1 \tag{9}$$

Rearranging:

$$N_w^s = \frac{1 - v_e \left(\frac{\Gamma_e^{(w)}}{\delta} \right)}{v_w + v_e \left(\frac{x_e^b}{1 - x_e^b} \right)} \tag{10}$$

And the molar fraction at the surface is then:

$$x_e^s = \frac{\frac{\Gamma_e^{(w)}}{\delta} + \frac{x_e^b}{1-x_e^b} N_w^s}{\left(\frac{\Gamma_e^{(w)}}{\delta} + \frac{x_e^b}{1-x_e^b} N_w^s \right) + N_w^s} \quad (11)$$

The above equation links the surface concentration to the Gibbs excess, $\Gamma_e^{(w)}$, at any given x_e^b and δ.

The thickness, δ, cannot be determined experimentally. In the literature, the value of δ has been often assumed constant, for example at 5 Å for all ethanol/water mixtures [14]. As shown by thermodynamic analyses, the assumption of a constant thickness is no longer valid. In this study, x_e^s is determined via simulation as a function of x_e^b. The surface adsorption, $\Gamma_e^{(w)}$, is determined experimentally from neutron reflectometry. The combined NR and simulation results, x_e^s and $\Gamma_e^{(w)}$, are then applied to eq.(11) to determine δ via numerical iterations. The results are used to verify, or otherwise, the proposed relationship between the interfacial thickness and bulk concentration.

METHODOLOGY

Experimental

Heavy ethanol (d-ethanol, grade greater than 99.5%) and deuterated water (D_2O, grade greater than 99.9%) were purchased from Wako Pure Chemical and used without further purification. Solutions of heavy ethanol were prepared in a mixture of D_2O and H_2O (Milli-Q water) with the quantities of heavy and light water adjusted for each mixture to produce solutions with zero bulk reflection as described in the literature, determined through eq. (12). The reflectivity of six samples

was measured using the *SOFIA* reflectometer [18–20] at the Japan Accelerator Research Complex (J-PARC). The surface excess of ethanol was obtained by fitting the reflectivity profiles using *MOTOFIT* [21] and eq. (15) in the following section. All experimental studies were carried out at 25 °C.

NR analysis

It is possible to quantify the surface concentration of deuterated surfactants by exploiting the difference in scattering between the liquid bulk and the interface. The background reflectivity can be negated by utilising appropriate concentrations of D_2O and H_2O in the solvent, such that the positive and negative scattering cancels out. The overall scattering of a mixed solution (ρ) can be calculated from the contributions of each species in the mixture through eq.(12).

$$\rho = \sum_{i=1}^{n} x_{vi} SLD_i \tag{12}$$

In the above equation, x_i stands for the molar fractions of species *i*, and the scattering length density SLD_i (Å^{-2}) is given by eq.(13), where $\sum b_c$ is the sum of the bound coherent scattering of the atoms in each molecule and v_m is the molecular volume.

$$SLD_i = \frac{\sum b_c}{v_m} \tag{13}$$

Table 1. Scattering length densities of the molecules in solution

Scattering length density (SLD) ×Å^2	
Water	-0.56×10^{-6}
Heavy water	6.34×10^{-6}
Ethanol	-0.35×10^{-6}
Heavy ethanol	6.08×10^{-6}

Targeting zero bulk scattering imposes a maximum concentration of heavy ethanol, which, like D_2O, also has positive scattering. This maximum concentration occurs when the positive scattering of heavy ethanol is completely matched by the negative scattering of pure water:

$$\rho_b = 6.08\times10^{-6}(x_e^b) - 0.56\times10^{-6}(1-x_e^b) = 0 \qquad (14)$$

For a strong surfactant, the required bulk concentration is very low and has negligible effect on the D_2O concentration required to nullify the bulk reflection. Conversely, for ethanol, the bulk concentration is relatively high. As a result, the concentration of D_2O required to nullify the bulk solution is significantly affected by the concentration of d-ethanol. In this study, we used fully deuterated ethanol and restricted the bulk concentration to 3% to maintain a high interfacial contrast.

The NR data was analysed using the commercial software *MOTOFIT* [21]. Assuming a single interfacial layer, the overall scattering (ρ) and correction for background scattering (ρ_b) were optimised for a layer thickness (δ). Initial values of δ were estimated from molecular dynamics simulations, assuming a normal distribution for the ethanol peak and setting the interfacial boundaries at three standard deviations from the mean. Note that this is not the final interfacial thickness but serves only as a reasonable estimate for the initial analysis of the NR data.

Given the interfacial thickness (δ) and the total scattering of the interfacial layer ($\rho-\rho_b$), the effective area per molecule in the film (A) and the Gibbs excess concentration ($\Gamma_e^{(w)}$) are associated through eq(15), where again, $\sum b_c$ is the sum of the scattering lengths across an ethanol molecule and N_a is Avogadro's number [22]. The term $(\rho-\rho_b)\delta$ was not significantly

affected by small changes to the interfacial thickness during analysis with MOTOFIT, as the scattering density would reduce accordingly.

$$A = \frac{\sum b_c}{(\rho - \rho_b)\delta} = \frac{1}{\Gamma_e^{(w)} N_a} \qquad (15)$$

The Gibbs excess concentration can then be related to the surface concentration via eq. (11) for a given δ. In this work, the interfacial thickness was first estimated by molecular simulations prior to analysis in *MOTOFIT*.

Simulation

The vacuum/solution (d-ethanol and water) interface was created by placing a slab of solution (~10 nm thickness) between two empty regions of 10 nm length each, as shown in **Figure 1**.

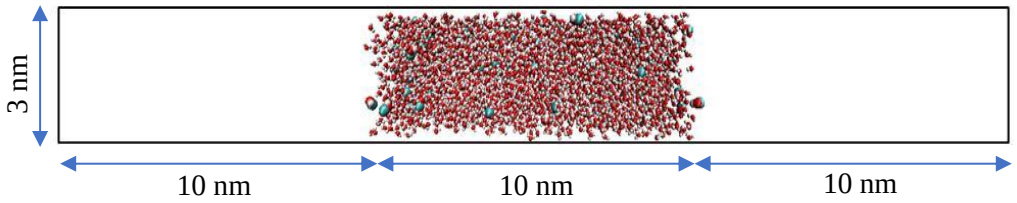

Figure 1. Simulation box: H and D – white, O – red, C - blue.

Molecular trajectories with a time step of 1 fs were generated using GROMACS 4.5.5.[23] Water molecules were modelled by SPC/E [24]. The molecular potential for d-ethanol was described by the GROMOS96 force field [25–27]. The charge distribution of the hydroxyl group was gathered from the literature,[28] and has been used previously with success [29]. All deuterium atoms were united with their corresponding carbon atom, except those in the hydroxyl groups.

The simulation box was set up according to standard procedures [30]. Firstly, a number of d-ethanol molecules were put into a 3×3×10 nm box. The remaining space in the box then was filled

up with water molecules. The simulation was performed at constant temperature (298 K) and pressure (1 bar) using a Berendsen barostat [31] with a cut-off of 1.3 nm and a relaxation time of 2 ps. Consequently, the two dimensions, *x*- and *y*-, of the box were adjusted appropriately, while the z-dimension was extended to 30 nm to form two empty regions as shown in **Figure 1**. These paired vacuum/solution interfaces have been widely used to simulate the air/water interface [32]. Finally, the simulation was performed for 20 ns at constant volume and temperature (298 K) using the Nose-Hoover thermostat. Analysis of the density distribution, surface tension and water dipole moment was performed on the last 10 ns. The bond lengths of the alcohol molecules and the geometry of the water molecules were unchanged, according to LINCS algorithms [33]. The electrostatic interactions were regulated using Ewald sums [34]. The trajectories were recorded for analysis every 500 fs [35]. From the density profiles, the bulk and interfacial composition were calculated. An example of the density profiles is given in Figure 2.

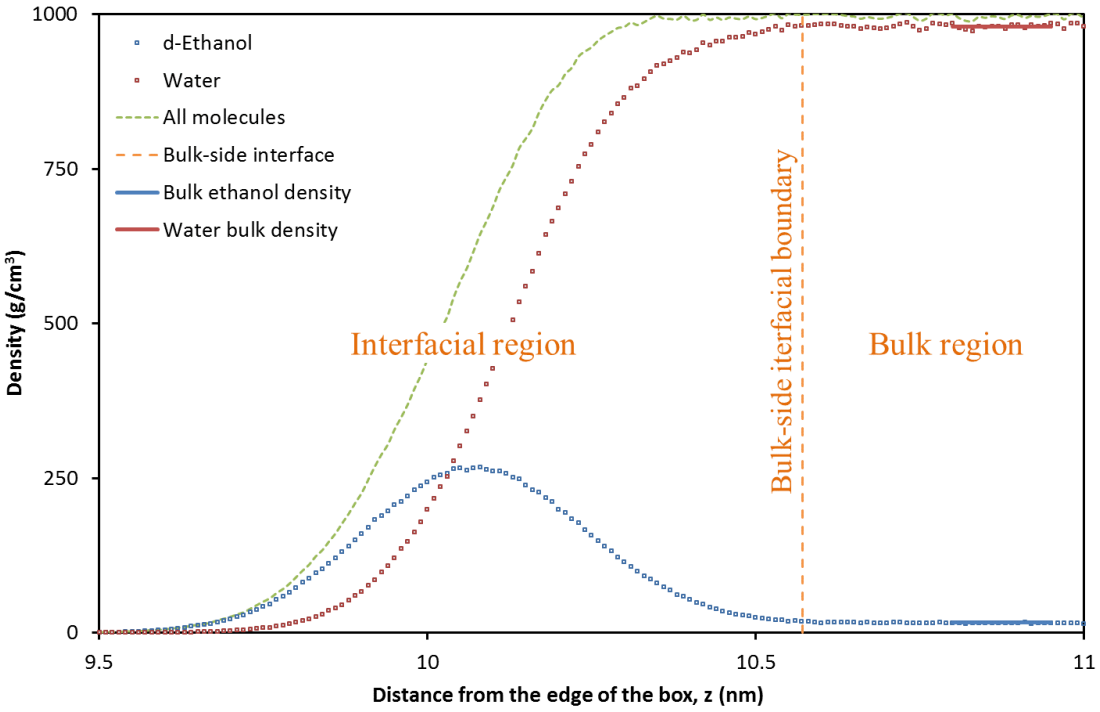

Figure 2. Density distributions of species in the interfacial zone of the ethanol/water/air interface.

RESULTS AND DISCUSSION

Interfacial concentration

NR analysis was conducted over a bulk ethanol concentration of 0 to 4%. The Gibbs excess concentration determined by NR analysis exceeded the 0.8×10^{-6} mol/m^2 that had long been associated with the theoretical maximum (monolayer) coverage of any alcohol at the interface [5]. This finding is consistent with a recent thermodynamic study[13] which reports Gibbs excess values in excess of this monolayer coverage and increasing with the length of the alcohol. This higher excess concentration implies strongly that the water-alcohol interface is not a simple monolayer with the maximum coverage determined by the size of the head group, a fact supported by the larger interfacial thicknesses reported in the study. The interfacial concentrations determined for each solution are shown in Figure 3.

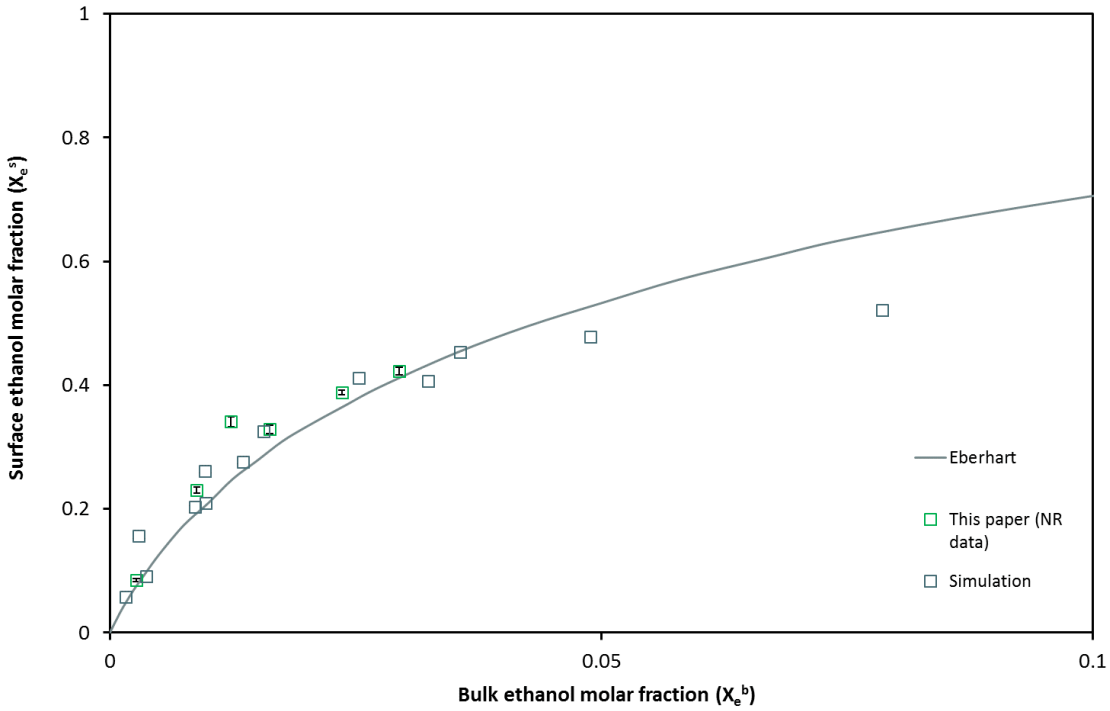

Figure 3. The relationship between bulk and interfacial concentrations, calculated from the simulation (grey squares) and using the fitted thickness with NR data (green squares).

The solution concentrations, scattering and calculated Gibbs excess are shown in Table 2 below.

Table 2. Properties and concentrations of the bulk solutions, including scattering $(\rho_s - \rho_b)\delta$, from Motofit and Gibbs excess (from equation (15)). Volumetric properties of the solutions are estimated from the data of González et al, assuming that the mixing of heavy ethanol and heavy water follows the same empirical relationship as normal ethanol in water.

	$(\rho-\rho_b)\delta$			$\Gamma_e^{(w)}$	Bulk compositions				
#	×10⁶ Å⁻¹			×10⁶ mol/m2	m% (EtOH)	n% (EtOH)	n% (D_2O)	v% (EtOH)	v% (D_2O)
A	36.06	+/-	0.17	10.15	8.22%	3.00%	0.00%	8.55%	0.00%
C	26.52	+/-	0.14	7.46	3.37%	1.20%	4.54%	3.53%	4.43%
D	24.54	+/-	0.15	6.91	0.76%	0.27%	7.84%	0.79%	7.80%
E	34.15	+/-	0.17	9.61	6.52%	2.36%	1.20%	6.79%	1.15%
F	30.58	+/-	0.15	8.60	4.53%	1.62%	3.42%	4.73%	3.31%
G	29.80	+/-	0.15	8.38	2.49%	0.88%	5.56%	2.61%	5.46%

To further verify the consistency of the simulations, the surface tension reduction at each concentration was compared with experimental data [6], as shown in Figure 4. It can be seen that the simulated values were consistent with experimental values, and similar to previous reports [36,37].

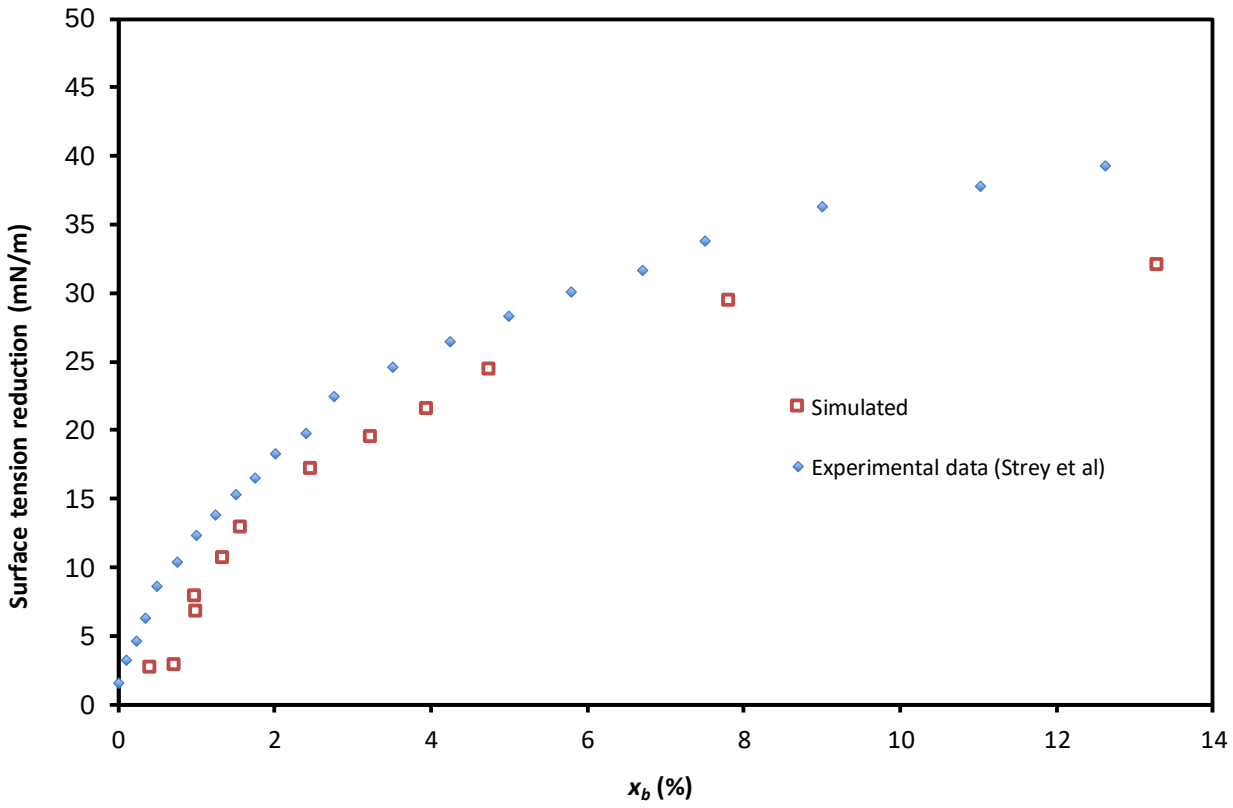

Figure 4. Surface tension reduction determined by simulation and measurement.

Interfacial thickness

Due to the difficulty of defining the interfacial boundaries, the interfacial thickness was not calculated directly from the molecular simulations. Instead, the interfacial composition is determined from the molecular simulations through the region where the ethanol shows enrichment at the surface – this is defined by fitting a normal distribution to the ethanol molecular density and setting the bulk-side boundary at three standard deviations from the mean, as shown in Figure 2. The region from that point forward (to the air side) is considered part of the interface

and the interfacial concentration is calculated from the molecular densities in this region. However, it is not possible to define the air-side boundary directly due to the relative scale of surface roughness, ~ 3.2 Å [15]. This is the same issue as encountered when trying to measure the thickness directly.

The interfacial thickness is instead determined by combining this surface concentration (determined from the simulations) and the Gibbs excess determined from NR data, as there exists a unique value of interfacial thickness which will allow these two properties to be reconciled.

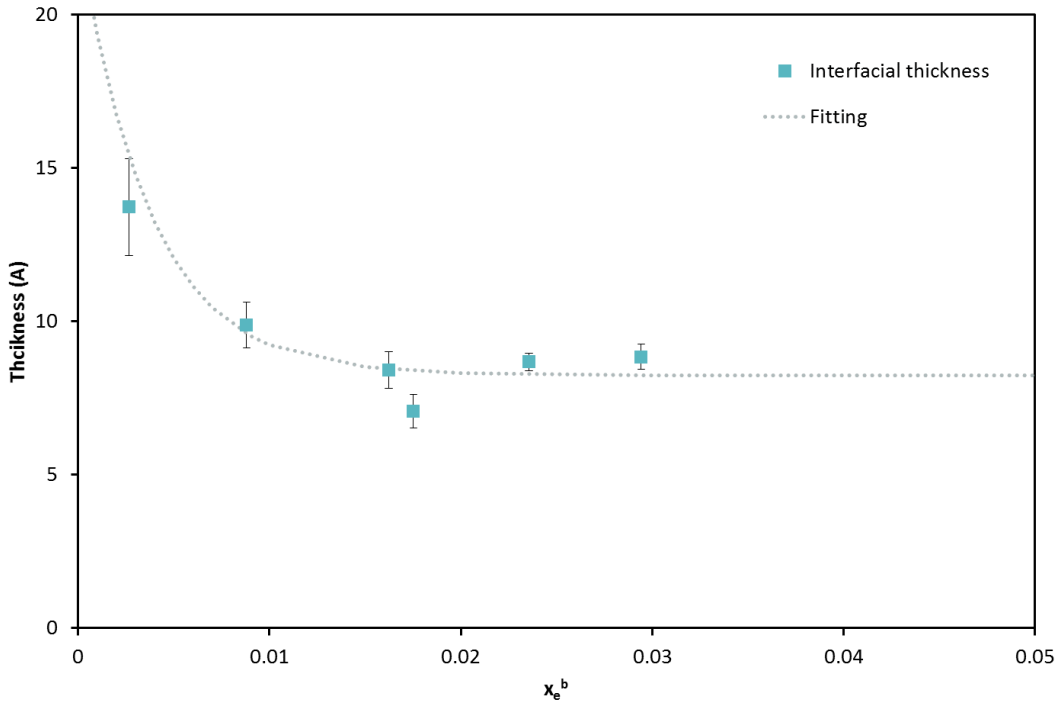

Figure 5. Interfacial thickness of the ethanol/water/air interface, determined by reconciling simulation and NR data.

Reconciliation between NR data and simulated x_e^s for each solution indicated a decreasing trend of δ as the solution concentration increased. The trend is similar to Bagheri's proposal [1], that

the interfacial thickness decreases in the form of exponential decay. The following equation relating the interfacial thickness to the bulk concentration is proposed:

$$\delta = \delta_0 \exp(\lambda\, x_e^b) + \delta_{inf} \quad (16)$$

where δ_0 and δ_{inf} are the theoretical limits at $x_e^b = 0$ and $x_e^b = 1$, respectively, and λ is the rate of decay.

Equation (16) was fitted to the data, giving $\delta_0 = 14.6$ Å, $\delta_{inf} = 8.2$ Å and $\lambda = 296$. It can be seen that both thickness (Figure 5) and interfacial composition (Figure 3) are consistently described by the model. Furthermore, at these low concentrations, the interfacial composition is also consistent with Eberhart's proposal [10].

The results show the interfacial thickness to be significantly larger than the estimated 5.5 Å used previously by Li et al.[14] In the literature, it has been shown that both hydroxyl and methyl groups of ethanol have distinctive hydration layers [38] and can disrupt the network of hydrogen bonds at the solution's surface.[39] As a result, the effective interfacial layer should include the hydration shells of the alcohol molecules, [40] making it larger than a lone ethanol molecule. Larger interfacial thicknesses are determined for particularly low concentrations (with 15 Å recorded for the 0.3% sample), where the degree of enrichment at the interface is greatest [1]. The thickness then tends to a limiting value of 8.2 Å in a trend that can be fitted to exponential decay. This is consistent with the work of Bagheri et al.[1], which reports a decrease from 13 to roughly 7 Å. In Figure 3, the interfacial concentrations calculated from the NR data using the fitted model of interfacial thickness are shown alongside the composition determined from the simulations. For comparison, the proposal of Eberhart [13], where the surface tension is made up of the surface

tensions of the pure components weighted by their relative concentrations in the interfacial layer, is also shown.

By combining surface tension data with thermodynamic theory, Bagheri et al[1] report a maximum Gibbs excess concentration just below 10×10^{-6} mol/m^2, well in excess of the predicted monolayer coverage. Furthermore, the maximum Gibbs excess increased with the length of the hydrocarbon tail. By Bagheri's analysis, the interfacial thickness was found to come rapidly to a maximum value of 13.2 Å before slowly reducing, tending towards a stable 7 Å. Azizian and Moghadam [41] found the interfacial thickness to decrease with increasing alcohol concentration. Our results in Figure 5 clearly confirm that the thickness decreases with increasing ethanol concentration. The deviations between this work and previous analyses may be due to the fact that the thermodynamic analysis was based solely on surface tension data.

CONCLUSION

It is the purpose of this study to augment the body of NR data for the ethanol-water system and to place that data amongst the myriad of models which attempt to predict surfactant behaviour. The combination of NR, molecular dynamics and theoretical analysis provides an objective determination of the interfacial thickness. The findings confirm that the interfacial thickness is not constant and instead decreases with increasing ethanol concentration. This result is consistent with a recent thermodynamic analysis and demonstrated the limitation of the conventional theory, which oversimplified the interfacial layer. The new insights provide a theoretical framework to describe the interfacial layer of water/alcohol mixtures.

ACKNOWLEDGEMENT

The neutron scattering experiment was approved by the Neutron Science Proposal Review Committee of J-PARC/MLF (Proposal No. 2016A0153). The simulation was supported by Pawsey Supercomputing Centre (Western Australia) through the use of advanced computing resources. A.H. was supported by an Australian Government Research Training Program Scholarship.

REFERENCES

[1] A. Bagheri, M. Fazli, M. Bakhshaei, Surface properties and surface thickness of aqueous solutions of alcohols, J. Mol. Liq. 224 (2016) 442–451. doi:10.1016/j.molliq.2016.09.113.

[2] M.S.C.S. Santos, J.C.R. Reis, Thermodynamic evaluation of molar surface area and thickness of water + ethanol mixtures, J. Mol. Liq. 255 (2018) 419–428. doi:10.1016/j.molliq.2018.01.136.

[3] I. Langmuir, The distribution and orientation of molecules, in: Third Colloid Symp. Monogr., 1925.

[4] A. Chodzińska, A. Zdziennicka, B. Jańczuk, Volumetric and surface properties of short chain alcohols in aqueous solution-air systems at 293 K, J. Solution Chem. 41 (2012) 2226–2245. doi:10.1007/s10953-012-9935-z.

[5] Y.F. Yano, Correlation between surface and bulk structures of alcohol-water mixtures, J. Colloid Interface Sci. 284 (2005) 255–259. doi:10.1016/j.jcis.2004.09.059.

[6] R. Strey, Y. Viisanen, M. Aratono, J.P. Kratohvil, Q. Yin, S.E. Friberg, On the Necessity of Using Activities in the Gibbs Equation, J. Phys. Chem. B. 103 (1999) 9112–9116. doi:10.1021/jp990306w.

[7] E.A. Guggenheim, N.K. Adam, The Thermodynamics of Adsorption at the Surface of Solutions, Proc. R. Soc. London. Ser. A. 139 (1933) 218–236.

[8] E.A. Guggenheim, Thermodynamics: an advanced treatment for chemists and physicists, North-Holland Pub. Co., 1949.

[9] M. Aratono, T. Toyomasu, M. Villeneuve, Y. Uchizono, T. Takiue, K. Motomura, N. Ikeda, Thermodynamic Study on the Surface Formation of the Mixture of Water and Ethanol, J. Colloid Interface Sci. 191 (1997) 146–53. doi:10.1006/jcis.1997.4929.

[10] J.G. Eberhart, The Surface Tension of Binary Liquid Mixtures1, J. Phys. Chem. 70 (1966) 1183–1186. doi:10.1021/j100876a035.

[11] A. Laaksonen, Nucleation of binary water–n-alcohol vapors, J. Chem. Phys. 97 (1992) 1983. doi:10.1063/1.463136.

[12] A.S. Wexler, C.S. Dutcher, Statistical mechanics of multilayer sorption: Surface tension, J. Phys. Chem. Lett. 4 (2013) 1723–1726. doi:10.1021/jz400725p.

[13] M. Salonen, J. Malila, I. Napari, A. Laaksonen, Evaluation of surface composition of surface active water-alcohol type mixtures: A comparison of semiempirical models, J. Phys. Chem. B. 109 (2005) 3472–3479. doi:10.1021/jp047610w.

[14] Z.X. Li, J.R. Lu, D.A. Styrkas, R.K. Thomas, A.R. Rennie, J. Penfold, The structure of the surface of ethanol/water mixtures, Mol. Phys. 80 (1993) 925–939. doi:10.1080/00268979300102771.

[15] A. Braslau, M. Deutsch, P.S. Pershan, A.H. Weiss, J. Als-Nielsen, J. Bohr, Surface Roughness of Water Measured by X-Ray Reflectivity, Phys. Rev. Lett. 54 (1985) 114–117.

doi:10.1103/PhysRevLett.54.114.

[16] C. Bermúdez-Salguero, J. Gracia-Fadrique, Gibbs excess and the calculation of the absolute surface composition of liquid binary mixtures, J. Phys. Chem. B. 119 (2015) 5598–5608. doi:10.1021/acs.jpcb.5b01436.

[17] B. González, N. Calvar, E. Gómez, Á. Domínguez, Density, dynamic viscosity, and derived properties of binary mixtures of methanol or ethanol with water, ethyl acetate, and methyl acetate at T = (293.15, 298.15, and 303.15) K, J. Chem. Thermodyn. 39 (2007) 1578–1588. doi:10.1016/j.jct.2007.05.004.

[18] K. Mitamura, N.L. Yamada, H. Sagehashi, H. Seto, N. Torikai, T. Sugita, M. Furusaka, A. Takahara, Advanced Neutron Reflectometer for Investigation on Dynamic/Static Structures of Soft-Interfaces in J-PARC, Futur. Trends Soft Mater. Res. with Adv. Light Sources. 272 (2011) 1–5. doi:Artn 012017\rDoi 10.1088/1742-6596/272/1/012017.

[19] K. Mitamura, N.L. Yamada, H. Sagehashi, N. Torikai, H. Arita, M. Terada, M. Kobayashi, S. Sato, H. Seto, S. Goko, M. Furusaka, T. Oda, M. Hino, H. Jinnai, A. Takahara, Novel neutron reflectometer SOFIA at J-PARC/MLF for in-situ soft-interface characterization, Polym J. 45 (2013) 100–108. http://dx.doi.org/10.1038/pj.2012.156.

[20] N.L. Yamada, N. Torikai, K. Mitamura, H. Sagehashi, S. Sato, H. Seto, T. Sugita, S. Goko, M. Furusaka, T. Oda, M. Hino, T. Fujiwara, H. Takahashi, A. Takahara, Design and performance of horizontal-type neutron reflectometer SOFIA at J-PARC/MLF, Eur. Phys. J. Plus. 126 (2011) 108. doi:10.1140/epjp/i2011-11108-7.

[21] A. Nelson, Co-refinement of multiple-contrast neutron/X-ray reflectivity data using {\it

MOTOFIT}, J. Appl. Crystallogr. 39 (2006) 273–276. doi:10.1107/S0021889806005073.

[22] K.L. Mittal, D.O. Shah, Adsorption and Aggregation of Surfactants in Solution, Taylor & Francis, 2002.

[23] B. Hess, C. Kutzner, D. van der Spoel, E. Lindahl, GROMACS 4: Algorithms for Highly Efficient, Load-Balanced, and Scalable Molecular Simulation, J. Chem. Theory Comput. 4 (2008) 435–447. doi:10.1021/ct700301q.

[24] F. Chen, P.E. Smith, Simulated surface tensions of common water models, J. Chem. Phys. 126 (2007) 221101. doi:10.1063/1.2745718.

[25] A.W. Schüttelkopf, D.M.F. van Aalten, PRODRG: a tool for high-throughput crystallography of protein-ligand complexes, Acta Crystallogr. Sect. D. 60 (2004) 1355–1363. doi:10.1107/S0907444904011679.

[26] W.R.P. Scott, P.H. Hünenberger, I.G. Tironi, A.E. Mark, S.R. Billeter, J. Fennen, A.E. Torda, T. Huber, P. Krüger, W.F. van Gunsteren, The GROMOS Biomolecular Simulation Program Package, J. Phys. Chem. A. 103 (1999) 3596–3607. doi:10.1021/jp984217f.

[27] J. Hermans, H.J.C. Berendsen, W.F. Van Gunsteren, J.P.M. Postma, A consistent empirical potential for water–protein interactions, Biopolymers. 23 (1984) 1513–1518. doi:10.1002/bip.360230807.

[28] W.L. Jorgensen, Optimized intermolecular potential functions for liquid alcohols, J. Phys. Chem. 90 (1986) 1276–1284. doi:10.1021/j100398a015.

[29] C. V Nguyen, C.M. Phan, H.M. Ang, H. Nakahara, O. Shibata, Y. Moroi, Molecular Dynamics Investigation on Adsorption Layer of Alcohols at the Air/Brine Interface,

Langmuir. 31 (2015) 50–56. doi:10.1021/la504471q.

[30] P. Jungwirth, D.J. Tobias, Specific Ion Effects at the Air/Water Interface, Chem. Rev. 106 (2006) 1259–1281. doi:10.1021/cr0403741.

[31] D.J. Evans, B.L. Holian, The Nose–Hoover thermostat, J. Chem. Phys. 83 (1985) 4069–4074. doi:10.1063/1.449071.

[32] V. Venkateshwaran, S. Vembanur, S. Garde, Water-mediated ion–ion interactions are enhanced at the water vapor–liquid interface, Proc. Natl. Acad. Sci. U. S. A. 111 (2014) 8729–8734. doi:10.1073/pnas.1403294111.

[33] B. Hess, H. Bekker, H.J.C. Berendsen, J.G.E.M. Fraaije, LINCS: A linear constraint solver for molecular simulations, J. Comput. Chem. 18 (1997) 1463–1472.

[34] M. Deserno, C. Holm, How to mesh up Ewald sums. II. An accurate error estimate for the particle-particle-particle-mesh algorithm, J. Chem. Phys. 109 (1998) 7694–7701. doi:10.1063/1.477415.

[35] D. van der Spoel, E. Lindahl, B. Hess, A. van Buuren, E. Apol, P. Meulenhoff, D. Tieleman, A. Sijbers, K. Feenstra, R. van Drunen, Gromacs User Manual version 4.5.4., 2010.

[36] F. Biscay, A. Ghoufi, P. Malfreyt, Surface tension of water-alcohol mixtures from Monte Carlo simulations, J. Chem. Phys. 134 (2011). doi:10.1063/1.3544926.

[37] C.M. Phan, C.V. Nguyen, T.T.T. Pham, Molecular Arrangement and Surface Tension of Alcohol Solutions, J. Phys. Chem. B. 120 (2016). doi:10.1021/acs.jpcb.6b01209.

[38] Y. Gong, Y. Xu, Y. Zhou, C. Li, X. Liu, L. Niu, Y. Huang, X. Zhang, C.Q. Sun, Hydrogen

bond network relaxation resolved by alcohol hydration (methanol, ethanol, and glycerol), J. Raman Spectrosc. 48 (2017) 393–398. doi:10.1002/jrs.5060.

[39] G. Gao, C. V. Nguyen, C.M. Phan, Molecular arrangement between electrolyte and alcohol at the air/water interface, J. Mol. Liq. 242 (2017) 859–867. doi:10.1016/j.molliq.2017.07.083.

[40] C.M. Phan, Independent Surface Action at the Air/Water Surface: a Renewed Concept via Artificial Neural Network, Colloids Surfaces A Physicochem. Eng. Asp. 567 (2019) 319–324. doi:10.1016/j.colsurfa.2019.01.024.

[41] S. Azizian, T.F. Moghadam, Derivation of a new equation for prediction of the thin layer depth of the extended-Langmuir model for dilute binary mixtures, Colloids Surfaces A Physicochem. Eng. Asp. 378 (2011) 67–71. doi:https://doi.org/10.1016/j.colsurfa.2011.01.055.